HHS Public Access

Author manuscript

Am J Surg Pathol. Author manuscript; available in PMC 2017 April 01.

Published in final edited form as:

Am J Surg Pathol. 2016 April ; 40(4): 433–442. doi:10.1097/PAS.0000000000000591.

Novel *BCOR-MAML3* and *ZC3H7B-BCOR* Gene Fusions in Undifferentiated Small Blue Round Cell Sarcomas

Katja Specht[1], **Lei Zhang**[2], **Yun-Shao Sung**[2], **Marisa Nucci**[3], **Sarah Dry**[4], **Sumathi Vaiyapuri**[5], **Gunther HS Richter**[6], **Christopher DM Fletcher**[3], and **Cristina R Antonescu**[2]

[1]Department of Pathology, Technische Universität München, Munich, Germany

[2]Department of Pathology, Memorial Sloan Kettering Cancer Center, New York, NY

[3]Department of Pathology, Brigham and Women's Hospital, Boston, MA

[4]Department of Pathology, UCLA, Los Angeles, CA

[5]Department of Pathology, Royal Orthopaedic, Birmingham, UK

[6]Children's Cancer Research Center and Department of Pediatrics, Klinikum rechts der Isar, Technische Universität München, and Comprehensive Cancer Center Munich (CCCM), Munich, Germany

Abstract

Small blue round cell tumors (SBRCTs) are a heterogenous group of tumors that are difficult to diagnose due to overlapping morphologic, immunohistochemical and clinical features. About two-thirds of *EWSR1*-negative SBRCTs are associated with *CIC-DUX4* related fusions, while another small subset shows *BCOR-CCNB3* X-chromosomal paracentric inversion. Applying paired-end RNA sequencing to an SBRCT index case of a 44 year-old male, we identified a novel *BCOR-MAML3* chimeric fusion, which was validated by RT-PCR and FISH techniques. We then screened a total of 75 SBRCTs lacking *EWSR1, FUS, SYT, CIC* and *BCOR-CCNB3* abnormalities, for *BCOR* break-apart probes by FISH to detect potential recurrent *BCOR* gene rearrangements, outside the typical X-chromosomal inversion. Indeed, 8/75 (11%) SBRCTs showed distinct *BCOR* gene rearrangements, with 2 cases each showing either a *BCOR-MAML3* or the alternative *ZC3H7B-BCOR* fusion, while no fusion partner was detected in the remaining 4 cases. Gene expression of the *BCOR-MAML3* positive index case showed a distinct transcriptional profile with upregulation of *HOX*-gene signature, compared to classic Ewing sarcoma or *CIC-DUX4*-positive SBRCTs. The clinicopathologic features of the SRBCTs with alternative *BCOR* rearrangements were also compared with a group of *BCOR-CCNB3* inversion positive cases, combining 11 from our files with a meta-analysis of 42 published cases. The *BCOR-CCNB3*-positive tumors occurred preferentially in children and in bone, in contrast to alternative *BCOR*-rearranged SBRCTs which presented in young adults, with a variable anatomic distribution. Furthermore *BCOR*-rearranged tumors often displayed spindle cell areas, either well-defined in intersecting fascicles or blending

Corresponding Authors: Cristina R Antonescu, MD, Memorial Sloan-Kettering Cancer Center, Pathology Department, 1275 York Ave, New York, NY, Phone: (212)639-5905; antonesc@mskcc.org and Christopher D Fletcher, Brigham and Women's Hospital, Boston, MA, cfletcher@partners.org.

Conflicts of interest: none

with the round cell component, which appears distinct from most other fusion-positive SBRCTs and shares histologic overlap with poorly differentiated synovial sarcoma.

Keywords

small blue round cell tumor; *BCOR-MAML3*; *ZC3H7B-BCOR*; Ewing Sarcoma

INTRODUCTION

The differential diagnosis of primitive small blue round cell tumors (SBRCTs) poses a challenge to both pathologists and clinicians due to overlapping morphologic, immunohistochemical and clinical features. Ewing sarcoma (ES) is the prototypical SBRCT molecularly characterized by canonical fusions between *EWSR1* and a gene of the *ETS* family of transcription factors. The molecular landscape of SBRCTs with Ewing-like morphology has been further expanded by the discovery of fusions of *EWSR1* with alternative non-*ETS* partners[1], with *EWSR1-NFATc2* fusion being one of the more common events in this class, being associated with amplification of the fusion transcript. [2]

Another subset of SBRCTs sometimes referred to as ‘ES-like’ or ‘atypical ES’ are sarcomas with *CIC-DUX4* fusion resulting from either a t(4;19)(q35;q13) or a t(10;19)(q26;q13).[3–6] The *CIC-DUX4* fusion appears functionally unrelated to *EWSR1-ETS* and the reported distinct gene signature and immunoprofile of *CIC-DUX4* sarcomas suggest a pathogenesis distinct from ES.[3,7] The morphologic appearance of *CIC-DUX4*-sarcomas is less monotonous compared to classic ES, with slight nuclear pleomorphism, vesicular chromatin with focally prominent nucleoli, more abundant cytoplasm, areas of spindling and myxoid matrix.[6,8] Clinically, *CIC-DUX4*-positive tumors are highly aggressive, arising almost exclusively in deep soft tissue of young adults.

More recently, Pierron et al[9] identified a fusion between *BCOR* (encoding the BCL6 transcriptional co-repressor) and *CCNB3* (encoding the testis-specific cyclin B3) in SBRCTs with ES-like morphology, resulting from an X-chromosomal paracentric inversion, which links the *BCOR* coding sequence to the *CCNB3* exon 5. Although *BCOR-CCNB3* positive SBRCTs share with ES certain similarities, such as clinical presentation often in bone and some morphologic and immunohistochemical overlap [10–12], they show a distinct gene expression profile and copy number changes compared to classic ES.[9]

Whether these newly identified genetic entities represent stand-alone categories of tumors or should be subsumed under the ES family of tumors is still a matter of debate. At present, the number of reported cases carrying a *CIC-DUX4* or *BCOR-CCNB3* fusion is still limited. Nevertheless, distinction of these SBRCT subsets appears important from a clinical and therapeutic point of view, to allow prospective therapeutic management with selection of proper chemotherapeutic regimens or target-specific therapy.[13]

In this study, we attempted to further characterize the molecular spectrum of ES-like tumors using next generation RNA sequencing for novel gene fusion discovery in an index case.

Subsequently validated abnormalities were then screened in a large cohort of primitive unclassified SBRCTs negative for *EWSR1/FUS/SYT/CIC*-related fusions.

MATERIALS AND METHODS

The personal consultation files of the corresponding authors (CRA, CDF) and the Pathology files of Memorial Sloan Kettering Cancer Center, New York, NY (CRA) and the Technische Universität München, Germany (KS) were searched for cases with a diagnosis of SBRCT or Ewing sarcomas, with tissue available for further immunohistochemical and molecular analysis. A total of 86 SBRCTs lacking *EWSR1, FUS, SYT* and *CIC* gene rearrangements were identified. From these 11 cases (13%) were positive for the *BCOR-CCNB3* paracentric inversion. The remaining 75 cases represented our study group. In one of these cases (SBRCT1) there was available frozen tissue for RNA sequencing and gene fusion detection. Morphology and previously performed immunohistochemical stains were reviewed in all cases. All cases were handled in accordance with the ethical rules of the respective institutions.

RNA sequencing

Total RNA was prepared from the index case for RNA sequencing according to the Illumina mRNA sample preparation protocol (Illumina). Briefly, mRNA was isolated with oligo(dT) magnetic beads from total RNA (10 μg) extracted from fresh-frozen tissue. Fragmentation of mRNA was performed at 94°C for 2.5 min in fragmentation buffer (Illumina). Prior to the adapter ligation step, an additional size-selection step (capturing 350–400 bp) was introduced to reduce inclusion of artifactual chimeric transcripts due to random priming of transcript fragments into the sequencing library.[14] Enrichment of the adapter-ligated library was achieved by PCR for 15 cycles. After purification, the library was sized and quantified using DNA1000 Kit (Agilent) on an Agilent 2100 Bioanalyzer according to the manufacturer's instructions. Paired-end RNA-sequencing at read lengths of 50 to 51 bp was performed with the HiSeq 2500 (Illumina). A total of about 97 million paired end reads were generated, corresponding to about 9.7 billion bases.

Analysis of RNA Sequencing Results with FusionSeq

Reads were independently aligned with STAR alignment software against the human genome reference sequence (hg19) and a splice junction library, simultaneously.[15] After conversion of mapped reads into Mapped Read Format,[16] analysis was performed using FusionSeq.[17] FusionSeq is a computational method that has been successfully applied to paired-end RNA-seq data for the identification of chimeric fusion transcripts.[9,18–20] Briefly, in a first step, paired end reads mapping to different genes were used to identify potential chimeric candidates. A cascade of filters, each taking into account different sources of noise in RNA-sequencing experiments, was then applied to remove spurious fusion transcripts. After generation of a confident list of fusion candidates, they were ranked to prioritize experimental validation.[17]

Interphase Fluorescence in situ Hybridization (FISH)

FISH analysis was performed on interphase nuclei from paraffin-embedded 4 μm sections applying bacterial artificial chromosomes (BAC clones), flanking *BCOR* on chromosome Xp11.4, *MAML3* on chromosome 4q31.1, *ZC3H7B* on chromosome 22q13 [20] and *CCNB3* on chromosome Xp11.22 (Supplementary Table 1). BAC clones were chosen according to the UCSC genome browser (http://genome.ucsc.edu) and were obtained from BACPAC sources of Children's Hospital of Oakland Research Institute (CHORI) (Oakland, CA) (http://bacpac.chori.org). DNA was isolated, labeled with different fluorochromes in a nick translation reaction, denatured and hybridized to pretreated slides as described previously. Two hundred tumor nuclei were evaluated using a Zeiss fluorescence microscope (Zeiss Axioplan, Oberkochen, Germany), controlled by Isis 5 software (Metasystems). A cut-off of >20% nuclei showing a break-apart signal was considered to be positive for rearrangement. Nuclei with incomplete set of signals were omitted from the score.

Reverse Transcription Polymerase Chain Reaction (RT-PCR)

An aliquot of the RNA extracted above from frozen tissue (Trizol Reagent; Invitrogen; Grand Island, NY) was used to confirm the fusion transcript identified by FusionSeq. RNA quality was determined by Eukaryote Total RNA Nano Assay and cDNA quality was tested for PGK housekeeping gene (247 bp amplified product). One microgram of total RNA was used for cDNA synthesis by SuperScript ® III First-Strand Synthesis Kit (Invitrogen, Carlsbad, CA). RT-PCR was performed using the Advantage-2 PCR kit (Clontech, Mountain View, CA) for 32 cycles at an annealing temperature of 64°C. The primers used were as follows: *BCOR* Exon 15 Fwd: 5'-GTCCTCCCGCATATTTCGC-3'; *MAML3* Exon 2 Rev: 5'-CCTGAAACCTTCTTTGCCCTTG-3'. Amplified products were purified and sequenced by Sanger method.

Gene Expression Profiling

Total RNA from fresh-frozen tissue extracted from SBRCT1 harboring a *BCOR-MAML3* fusion was labeled and hybridized onto an Affymetrix Human Gene 1.0 ST array (32,000 transcripts). The transcriptional profile was then compared with the expression of a large spectrum of normal tissues (n=16), studied on the same platform. The transcriptional signature was further compared to a previously published comprehensive gene expression meta-analysis of ES and *CIC-DUX4*-fusion positive SBRCTs.[7]

For data analysis, RMA-normalization was performed, including background correlation, quantile normalization, and median polish summary method.[21] Subsequent analysis was carried out with signal intensities that were log2-transformed to remove biases based on signal expression values.[22] Statistical t-test and FDR were performed to identify differentially expressed gene list, and subsequent hierarchical clustering was accomplished by heatmap function in R and bioconductor.[23] Annotation files for Affymetrix Human Gene arrays were obtained from Affymetrix website (http://www.affymetrix.com/support/technical/annotationfilesmain.affx) and analyzed using PERL script in order to match the probe IDs. Subsequently, gene set enrichment analysis (GSEA) was performed for investigating statistical associations between variable gene sets and phenotype of interest.[24] The algorithm in GSEA calculates the enrichment score, with corresponding significance

level based on permutation tests (empirical p-values and FDRs controlling global false positives). Each sample group was permutated 1,000 times to yield statistical significances.

RESULTS

The index case was that of a 44 year-old male patient who presented with a large intra-abdominal mass, clinically refractory to chemo- and radiotherapy (Figs. 1A, B and C). Morphologically, the tumor was classified in the ES family of tumors, showing sheets of primitive round to ovoid cells set in a slightly collagenized background (Fig. 1D). Tumor cells displayed finely stippled chromatin, scant eosinophilic cytoplasm, mild pleomorphism and a high mitotic rate (Fig 1E). After chemotherapy, there was no significant tumor response in the form of stromal fibrosis or changes in cytomorphology (Fig 1F). Immunohistochemically, strong CD99 membranous positivity was noted (Fig 1G). The tumor lacked the pathognomonic gene fusions characteristic for ES, namely *EWSR1* and *FUS*, and was also negative for *CIC* rearrangement and *BCOR-CCNB3* inversion by FISH.

FusionSeq data analysis identified a *BCOR-MAML3* fusion as the top candidate. Alignment of the reads suggested a fusion of *BCOR* exon 15 to *MAML3* exon 2 (Figs. 2A,B), a transcript that was subsequently confirmed by RT-PCR (Fig. 2C). The RNAseq further showed significant upregulation of both *BCOR* and *MAML3* mRNAs, compared to other translocation-positive sarcomas (Fig. 2D). As predicted from the structure of the chimeric *BCOR-MAML3* fusion, only *MAML3* exons 2–6 were significantly upregulated in the index case, but not in the other sarcomas (Fig. 2D).

Two recurrent *BCOR*-related fusions are identified in SBRCT: involving *MAML3* and *ZC3C7B* partner genes

To further confirm the *BCOR-MAML3* fusion at the genomic level, FISH experiments were conducted using custom BAC probes flanking the centromeric and telomeric regions of *BCOR* and *MAML3*, respectively. A break-apart split signal was seen in both *BCOR* (Fig. 3A) and *MAML3* (Fig. 3B) genes. A 3-color fusion FISH assay was also used confirming the co-localization of *BCOR* (red) with *MAML3* (yellow, centromeric) and the split of the green (telomeric) and yellow (centromeric) *MAML3* (Fig. 3C).

Among the 75 SBRCTs negative for all known fusions, such as *EWSR1*, *FUS*, *SYT*, *CIC* and the *BCOR-CCNB3* inversion, a total of 8 (11%) tumors showed other *BCOR* gene rearrangements using the *BCOR* break-apart FISH assay (Table 1). The subsequent FISH screening for potential partners identified *BCOR-MAML3* fusion in an additional case, while the remaining 6 cases showed no abnormalities in *MAML3*. Upon review of the literature for additional *BCOR* gene partners we identified *ZC3H7B* as a potential candidate, having been described in *BCOR-ZC3H7B* fusions in other sarcomas [20,25]. Thus we screened the remaining 6 *BCOR*-rearranged cases for *ZC3H7B* gene break-apart by FISH and found 2 positive cases. One of the cases showed an unbalanced *ZC3H7B* break-apart with deletion of the telomeric signal (SBRCT4, Supplementary Fig. 1), while the other showed a balanced *ZC3H7B* rearrangement (SBRCT3, data not shown). In the remaining 4 *BCOR*-rearranged cases no gene partner was identified.

Clinicopathologic Characteristics of *BCOR* rearranged SBRCTs (excluding *BCOR-CCNB3* positive cases)

All patients except one were male, with a mean and median age at diagnosis of 35 years and 39 years, respectively (range 5–70 years). Three cases arose in somatic soft tissue (upper extremity, groin/thigh, lower leg)(Supplementary Fig. 1), 2 intra-abdominal/pelvic, 2 cases in bone (ilium and skull base) and one tumor originated in the lung. Tumor size tended to be large (mean 13 cm). Based on the limited clinical data available (Table 1), most patients followed an aggressive clinical course, despite intensive radio- and/or chemotherapy therapy.

On microscopic examination, the *BCOR-MAML3* and *BCOR-ZC3H7B* positive tumors were characterized by a solid growth of undifferentiated cells, (Fig. 1D) often exhibiting infiltrative borders into adjacent anatomic structures, such as skeletal muscle or adipose tissue. The tumors were composed of a proliferation of primitive and relatively monomorphic small to medium-sized cells, with scant amphophilic or lightly eosinophilic cytoplasm, round to oval nuclei, with minor variation in size and shape (Figs. 1D). All except two cases showed a spindle cell component either arranged in intersecting fascicles, reminiscent of herring-bone growth pattern (Fig. 4A–C), or in a less defined, storiform or patternless growth. The spindle cell areas varied significantly from case to case either from being focal to comprising >30% of the tissue examined. In the remaining two cases lacking a distinct spindle cell component, the round cell component blended with cells that showed more oval to short spindled morphology. Areas of myxoid or edematous stromal change was also noted (Fig. 4E). Geographic tumor necrosis was common and prominent in the majority of cases, with frequent apoptosis and individual tumor cell necrosis (Fig. 4F). No rosette formation was observed.

Immunohistochemical Findings

The results of the immunohistochemical findings are summarized in Table 2. CD99 staining was seen in 6/7 *BCOR*-rearranged cases tested, but was quite variable being strong and diffuse only in the index case (Fig. 1G, Table 2), while being weak and patchy in the remaining lesions. One case was completely negative for CD99. Positivity for Cytokeratins (1/8) and Desmin (1/8) was rarely seen. All cases were negative for S100 protein and WT1, and one case tested was negative for CCNB3 (SBRCT1; data not shown).

A Distinct Gene Expression Signature of *BCOR-MAML3* positive sarcoma

We first determined the *BCOR-MAML3* associated gene expression signature of the SBRCT1 index case by using the Affymetrix Human Gene 1.0 ST arrays in comparison to a wide spectrum of 16 normal tissues.[7] Thus a 645 gene-list of differentially expressed genes was identified (fold change, FC, >1.4). Interestingly, among the highest ranked upregulated genes there were a significant number of genes from the homeobox (HOX) family (Supplementary Fig. 2). Also part of the *BCOR-MAML3* signature was the upregulation of both *BCOR* and *MAML3* mRNA expression, which confirmed the RNA sequencing results of SBRCT1 (Fig. 2D).

Using the VENN diagram tool, the above *BCOR-MAML3* gene signature was compared with the previously defined *CIC-DUX* and *EWSR1-FLi1* transcriptional signatures [7], which revealed a limited overlap between these 3 SBRCTs genetic subsets (Supplementary Fig. 3). The poor correlation between the *BCOR-MAML3* gene signature and the clustering of both *CIC-DUX* and *EWSR1-FLI1* SBRCT subsets was further confirmed by GSEA analysis (Supplementary Fig. 3).

BCOR-CCNB3 positive SBRCTs have characteristic clinicopathologic features

Among 86 SBRCTs lacking *EWSR1, FUS, SYT* and *CIC* gene rearrangements initially tested for *BCOR* abnormalities using a FISH assay designed to detect the *BCOR-CCNB3* paracentric inversion, 11 cases (13%) were positive for the *BCOR-CCNB3* fusion. All except one were male, with a median age of 15 years-old (range 2–44, mean 15). In fact all except two cases occurred in children and originated in the bone. These findings are in keeping with the clinicopathologic features of the 42 cases obtained from the meta-analysis of published cases[9–12], showing a similar median age of 13 years at diagnosis, preferentially occurring in males and at bone locations (Table 3). These clinical findings are somewhat different from the other *BCOR*-rearranged SBRCTs, which had an older age at diagnosis (median of 39 years old) and a more variable anatomic distribution between bone, soft tissue and intra-abdominal/visceral.

DISCUSSION

Undifferentiated round cell sarcomas are a heterogenous group of tumors that often affect children and young adults. Correct classification is critical for patient management, as well-defined subtypes of ES-like tumors require specific therapeutic regimens. With current molecular testing applied in clinical practice an increasing number of SBRCTs are found to lack the canonical *EWSR1-FLI1* fusion typical of ES. This subset of *EWSR1*-fusion negative undifferentiated SBRCTs has become the focus of significant investigation and debate recently, as on one hand they share significant overlap at the morphologic, immunophenotypic and clinical levels with classic ES, but display different genetic signatures, complicating diagnosis and clinical management.

The present study further expands the genetic spectrum of SBRCTs, with two novel fusions *BCOR-MAML3* and *ZC3H7B-BCOR*, identified in cases that have remained unclassified after extensive immunohistochemical and molecular testing. The *BCOR-MAML3* fusion was identified by RNA sequencing in an index case of a round cell sarcoma, negative for *EWSR1, FUS* and *CIC*-related abnormalities. As seen with the *BCOR-CCNB3* [9], the entire coding sequence of *BCOR* is also represented in the *BCOR-MAML3* fusion transcript. The *BCOR* gene, located at Xp11.4, encodes a ubiquitously expressed transcriptional repressor that associates with the BCL6 oncoprotein and with a variety of histone modifying enzymes, resulting in direct gene silencing by a unique combination of epigenetic modifications [2627] *BCOR* has a key role in the regulation of early development, hematopoiesis[28] and mesenchymal stem cell function.[29] In human diseases, *BCOR* is targeted by both mutations and translocations: somatic *BCOR* mutations are implicated in a subset of acute myeloid leukemia[30], while germline *BCOR* mutations cause the oculo-facio-cardio-dental (OFCD)

X-linked syndrome[31], characterized by microphthalmia, congenital cataracts, dysmorphic appearance, radiculomegaly and cardiac and digital defects. Gene fusions involving *BCOR*, with either *CCNB3* or *ZC3H7B* partner genes, are involved in several translocation-associated mesenchymal lesions, such as *BCOR-CCNB3* ES-like sarcomas [9] and ossifying fibromyxoid tumor and endometrial stromal sarcoma, respectively.[20,25] The finding of identical chromosomal translocations in diverse pathologic and clinical entities such as SBRCT, endometrial stromal sarcoma and ossifying fibromyxoid tumor (OMFT) adds to the growing list of otherwise unrelated entities that share genetic abnormalities. Moreover, a *BCOR-RARA* fusion has been described in acute promyelocytic leukemia.[32]

The *BCOR* gene partner, *MAML3*, encodes for a member of the mastermind-like (MAML) family of transcriptional co-activators. They constitute a component of the Notch signaling pathway, an evolutionarily conserved pathway with roles in diverse biological processes such as cell proliferation, differentiation and survival.[33] A recurrent *PAX3-MAML3* fusion has been identified recently in a high percentage of biphenotypic sinonasal sarcoma (19/25 cases; 79%),[34] a low grade sarcoma characterized by neural and myogenic differentiation, preferentially occurring in the sinonasal area of middle-aged patients.[35] Similar with this fusion, the *BCOR-MAML3* transcript in our SBRCT1 contains the exons 2–5 of *MAML3*, which retains the transactivation domain, but loses the Notch-binding site of MAML3. Furthermore, the other *BCOR* gene partner, *ZC3H7B*, zinc finger CCCH domain-containing protein 7B, encodes for a nuclear protein that contains a tetratricopeptide repeat domain and interacts with the rotavirus non-structural protein NSP3 [36]. The ZC3H7B protein has several domains that are involved in protein–protein and protein–nucleic acid interactions and, particularly, in multiprotein complexes. Although neither of the two SBRCTs with *ZC3H7B* gene rearrangement identified by FISH had tissue available for RT-PCR and fusion transcript structure confirmation, one of the cases showed an unbalanced rearrangement which was in keeping with *ZC3H7B* as 5’ and *BCOR* as the 3’ partner (Supplementary Fig 1). The prior reported evidence of *ZC3H7B-BCOR* fusion in either endometrial stromal sarcoma or OFMT obtained from RNA sequencing [20,25] points to the 3’position of *BCOR*, based on both unbalanced FISH pattern and predominance of the *ZC3H7B-BCOR* isoform detected by RT-PCR in a subset of these cases. The reported transcripts to date suggest the *ZC3H7B* exon 10 being fused to either exon 7 or 8 of *BCOR*.

Comparing the transcriptional profile of the *BCOR-MAML3* positive index case with that of previously published gene signatures of *ES* and *CIC-DUX4*-positive sarcomas,[7] there was only limited transcriptional overlap of *BCOR-MAML3*, *EWSR1-FLI*-positive ES and *CIC-DUX4*-tumors. Interestingly, among the genes overlapping between *BCOR-MAML3* and *CIC-DUX4* was *ETV4*, belonging to the PEA subfamily of ETS transcription factors, although the levels of upregulation was significantly higher in the *CIC-DUX4*-positive tumors.[13] Genes overlapping between *BCOR-MAML3* and *EWSR1-FLI1* positive tumors included *NKX2-2*, *TYMS*, *TOP2A*, *EZH2* and *ITGB3BP*. Among the genes highly upregulated in the *BCOR-MAML3*-positive index case were transcription factors of the HOX/homeobox family (Supplementary Fig 2), important for development of the body plan for axis formation.[37] Intriguingly, BCOR was also shown to have a role in normal laterality

determination, as patients with OFCD syndrome triggered by *BCOR* germline mutations exhibit defective lateralization including dextrocardia, asplenia and intestinal malrotation [38].

Altogether, 8/75 (11%) of our cohort of SBRCTs were positive for a *BCOR* rearrangement using the *BCOR* break-apart FISH assay. In 2 cases each, *BCOR* was fused to either *MAML3* or *ZC3H7B* genes. Although the number of cases is small, clinicopathologic data indicate a wide age range (5–70 years), almost exclusive occurrence in male patients and distribution among bone and soft tissue sites. Tumor size tended to be large and the clinical data available indicated an aggressive clinical course with multiple metastases or local recurrence despite intensive chemo- and radiotherapy (Table 1). The morphology of the *BCOR*-rearranged SBRCTs consisted of primitive, undifferentiated cells with a round, oval to spindled cell appearance. The latter spindle cell component was present in variable degrees in most cases, either forming well-defined fascicles, reminiscent of the fibrosarcoma herring-bone growth, or more often as a vague streaming or patternless pattern. The nuclear features included fine, stippled chromatin and mild variability in size and shape. The stromal component was typically scant, but when discernible varied from delicate collagenous to fibromyxoid. Although CD99 staining was seen in most cases, it was typically weak and patchy.

Among the 85 SBRCTs of our cohort lacking *EWSR1, FUS, SYT* and *CIC* gene rearrangements, 11 cases (13%) were positive for the *BCOR-CCNB3* paracentric inversion, using a FISH assay specifically designed to detect the inversion. We reviewed the additional 42 cases of *BCOR-CCNB3*-positive SBRCTs from the literature (Table 3)[9–12], for a combined meta-analysis of 53 cases. The clinicopathologic data indicate predominant occurrence in males (M:F ratio, 4:1), a median age at diagnosis of 13 years (range 2–44), and preferential localization within bone (38/53; 72%). RT-PCR techniques for detection of *BCOR-CCNB3* fusions or CCNB3 immunohistochemistry are excellent and reproducible tools for diagnosis of these tumors.[9] neither techniques, however, is appropriate for detecting the alternative *BCOR-MAML3* or *ZC3H7B-BCOR* fusions; these instead must be identified by FISH techniques using *BCOR* specific break-apart BAC probes.

In summary, we identify recurrent *BCOR* gene rearrangements in 11% of SBRCTs lacking other genetic abnormalities. Among this novel subset, *BCOR-MAML3* and *ZC3H7B-BCOR* represent two novel alternative fusions, which have not previously been reported in SBRCTs. These fusions add to the growing list of fusion genes recurrently found in SBRCT with ES-like morphology, although they may have different pathogenetic mechanisms of tumorigenesis, as the *BCOR* gene participates either with its entire coding sequence (*BCOR-MAML3, BCOR-CCNB3*) or only with its 3'portion (*ZC3H7B-BCOR*) to the chimeric fusion. Additional functional studies are needed to dissect further the consequences of these different transcript structures. Tumors harboring *BCOR* gene rearrangement occur preferentially in young adults and have a wide anatomic distribution. Morphologically, these lesions show a monomorphic/primitive appearance, ranging from small blue cells to spindle cells arranged in intersecting fascicles or patternless growth. Immunohistochemical work-up is mostly non-contributory, with CD99 often being positive but with a weak and patchy distribution. The presence of alternating round and spindle cell components appears distinct from most other fusion-positive SBRCTs, and thereby displaying morphologic overlap with

a poorly differentiated synovial sarcoma. It remains to be seen whether the increasingly detailed pathologic subclassification of SBRCT can be matched by the development of more effective histotype/genotype-specific therapies in these aggressive tumors.

Supplementary Material

Refer to Web version on PubMed Central for supplementary material.

Acknowledgments

Supported in part by: Wilhelm-Sander Stiftung (KS); P50 CA140146-01 (CRA); Kristen Ann Carr Foundation (CRA).

REFERENCES

1. Antonescu C. Round cell sarcomas beyond Ewing: emerging entities. Histopathology. 2014; 64:26–37. [PubMed: 24215322]
2. Szuhai K, Ijszenga M, de Jong D, et al. The NFATc2 gene is involved in a novel cloned translocation in a Ewing sarcoma variant that couples its function in immunology to oncology. Clin Cancer Res. 2009; 15:2259–2268. [PubMed: 19318479]
3. Kawamura-Saito M, Yamazaki Y, Kaneko K, et al. Fusion between CIC and DUX4 up-regulates PEA3 family genes in Ewing-like sarcomas with t(4;19)(q35;q13) translocation. Hum Mol Genet. 2006; 15:2125–2137. [PubMed: 16717057]
4. Yoshimoto M, Graham C, Chilton-MacNeill S, et al. Detailed cytogenetic and array analysis of pediatric primitive sarcomas reveals a recurrent CIC-DUX4 fusion gene event. Cancer Genet Cytogenet. 2009; 195:1–11. [PubMed: 19837261]
5. Graham C, Chilton-MacNeill S, Zielenska M, et al. The CIC-DUX4 fusion transcript is present in a subgroup of pediatric primitive round cell sarcomas. Hum Pathol. 2012; 43:180–189. [PubMed: 21813156]
6. Italiano A, Sung YS, Zhang L, et al. High prevalence of CIC fusion with double-homeobox (DUX4) transcription factors in EWSR1-negative undifferentiated small blue round cell sarcomas. Genes Chromosomes Cancer. 2012; 51:207–218. [PubMed: 22072439]
7. Specht K, Sung YS, Zhang L, et al. Distinct transcriptional signature and immunoprofile of CIC-DUX4 fusion-positive round cell tumors compared to EWSR1-rearranged Ewing sarcomas: further evidence toward distinct pathologic entities. Genes Chromosomes Cancer. 2014; 53:622–633. [PubMed: 24723486]
8. Choi EY, Thomas DG, McHugh JB, et al. Undifferentiated small round cell sarcoma with t(4;19)(q35;q13.1) CIC-DUX4 fusion: a novel highly aggressive soft tissue tumor with distinctive histopathology. Am J Surg Pathol. 2013; 37:1379–1386. [PubMed: 23887164]
9. Pierron G, Tirode F, Lucchesi C, et al. A new subtype of bone sarcoma defined by BCOR-CCNB3 gene fusion. Nat Genet. 2012; 44:461–466. [PubMed: 22387997]
10. Cohen-Gogo S, Cellier C, Coindre JM, et al. Ewing-like sarcomas with BCOR-CCNB3 fusion transcript: a clinical, radiological and pathological retrospective study from the Societe Francaise des Cancers de L'Enfant. Pediatric blood & cancer. 2014; 61:2191–2198. [PubMed: 25176412]
11. Puls F, Niblett A, Marland G, et al. BCOR-CCNB3 (Ewing-like) sarcoma: a clinicopathologic analysis of 10 cases, in comparison with conventional Ewing sarcoma. Am J Surg Pathol. 2014; 38:1307–1318. [PubMed: 24805859]
12. Peters TL, Kumar V, Polikepahad S, et al. BCOR-CCNB3 fusions are frequent in undifferentiated sarcomas of male children. Mod Pathol. 2015; 28:575–586. [PubMed: 25360585]
13. Sankar S, Lessnick SL. Promiscuous partnerships in Ewing's sarcoma. Cancer genetics. 2011; 204:351–365. [PubMed: 21872822]
14. Quail MA, Kozarewa I, Smith F, et al. A large genome center's improvements to the Illumina sequencing system. Nature methods. 2008; 5:1005–1010. [PubMed: 19034268]

15. Dobin A, Davis CA, Schlesinger F, et al. STAR: ultrafast universal RNA-seq aligner. Bioinformatics. 2013; 29:15–21. [PubMed: 23104886]
16. Habegger L, Sboner A, Gianoulis TA, et al. RSEQtools: a modular framework to analyze RNA-Seq data using compact, anonymized data summaries. Bioinformatics. 2011; 27:281–283. [PubMed: 21134889]
17. Sboner A, Habegger L, Pflueger D, et al. FusionSeq: a modular framework for finding gene fusions by analyzing paired-end RNA-sequencing data. Genome biology. 2010; 11:R104. [PubMed: 20964841]
18. Tanas MR, Sboner A, Oliveira AM, et al. Identification of a disease-defining gene fusion in epithelioid hemangioendothelioma. Science translational medicine. 2011; 3 98ra82.
19. Mosquera JM, Sboner A, Zhang L, et al. Recurrent NCOA2 gene rearrangements in congenital/infantile spindle cell rhabdomyosarcoma. Genes Chromosomes Cancer. 2013; 52:538–550. [PubMed: 23463663]
20. Antonescu CR, Sung YS, Chen CL, et al. Novel ZC3H7B-BCOR, MEAF6-PHF1, and EPC1-PHF1 fusions in ossifying fibromyxoid tumors--molecular characterization shows genetic overlap with endometrial stromal sarcoma. Genes Chromosomes Cancer. 2014; 53:183–193. [PubMed: 24285434]
21. Richter GH, Plehm S, Fasan A, et al. EZH2 is a mediator of EWS/FLI1 driven tumor growth and metastasis blocking endothelial and neuro-ectodermal differentiation. Proc Natl Acad Sci U S A. 2009; 106:5324–5329. [PubMed: 19289832]
22. Hauer K, Calzada-Wack J, Steiger K, et al. DKK2 mediates osteolysis, invasiveness, and metastatic spread in Ewing sarcoma. Cancer Res. 2013; 73:967–977. [PubMed: 23204234]
23. Antonescu CR, Yoshida A, Guo T, et al. KDR activating mutations in human angiosarcomas are sensitive to specific kinase inhibitors. Cancer Res. 2009; 69:7175–7179. [PubMed: 19723655]
24. Wang X, Cairns MJ. Gene set enrichment analysis of RNA-Seq data: integrating differential expression and splicing. BMC bioinformatics. 2013; 14(Suppl 5):S16. [PubMed: 23734663]
25. Panagopoulos I, Thorsen J, Gorunova L, et al. Fusion of the ZC3H7B and BCOR genes in endometrial stromal sarcomas carrying an X;22-translocation. Genes Chromosomes Cancer. 2013; 52:610–618. [PubMed: 23580382]
26. Gearhart MD, Corcoran CM, Wamstad JA, et al. Polycomb group and SCF ubiquitin ligases are found in a novel BCOR complex that is recruited to BCL6 targets. Mol Cell Biol. 2006; 26:6880–6889. [PubMed: 16943429]
27. Huynh KD, Fischle W, Verdin E, et al. BCoR, a novel corepressor involved in BCL-6 repression. Genes & development. 2000; 14:1810–1823. [PubMed: 10898795]
28. Wamstad JA, Corcoran CM, Keating AM, et al. Role of the transcriptional corepressor Bcor in embryonic stem cell differentiation and early embryonic development. PloS one. 2008; 3:e2814. [PubMed: 18795143]
29. Fan Z, Yamaza T, Lee JS, et al. BCOR regulates mesenchymal stem cell function by epigenetic mechanisms. Nature cell biology. 2009; 11:1002–1009. [PubMed: 19578371]
30. Grossmann V, Tiacci E, Holmes AB, et al. Whole-exome sequencing identifies somatic mutations of BCOR in acute myeloid leukemia with normal karyotype. Blood. 2011; 118:6153–6163. [PubMed: 22012066]
31. Ng D, Thakker N, Corcoran CM, et al. Oculofaciocardiodental and Lenz microphthalmia syndromes result from distinct classes of mutations in BCOR. Nat Genet. 2004; 36:411–416. [PubMed: 15004558]
32. Yamamoto Y, Tsuzuki S, Tsuzuki M, et al. BCOR as a novel fusion partner of retinoic acid receptor alpha in a t(X;17)(p11;q12) variant of acute promyelocytic leukemia. Blood. 2010; 116:4274–4283. [PubMed: 20807888]
33. McElhinny AS, Li JL, Wu L. Mastermind-like transcriptional co-activators: emerging roles in regulating cross talk among multiple signaling pathways. Oncogene. 2008; 27:5138–5147. [PubMed: 18758483]
34. Wang X, Bledsoe KL, Graham RP, et al. Recurrent PAX3-MAML3 fusion in biphenotypic sinonasal sarcoma. Nat Genet. 2014; 46:666–668. [PubMed: 24859338]

35. Lewis JT, Oliveira AM, Nascimento AG, et al. Low-grade sinonasal sarcoma with neural and myogenic features: a clinicopathologic analysis of 28 cases. Am J Surg Pathol. 2012; 36:517–525. [PubMed: 22301502]

36. Vitour D, Lindenbaum P, Vende P, et al. RoXaN, a novel cellular protein containing TPR, LD, zinc finger motifs, forms a ternary complex with eukaryotic initiation factor 4G and rotavirus NSP3. Journal of virology. 2004; 78:3851–3862. [PubMed: 15047801]

37. Wellik DM. Hox patterning of the vertebrate axial skeleton. Dev Dyn. 2007; 236:2454–2463. [PubMed: 17685480]

38. Hilton EN, Manson FD, Urquhart JE, et al. Left-sided embryonic expression of the BCL-6 corepressor, BCOR, is required for vertebrate laterality determination. Hum Mol Genet. 2007; 16:1773–1782. [PubMed: 17517692]

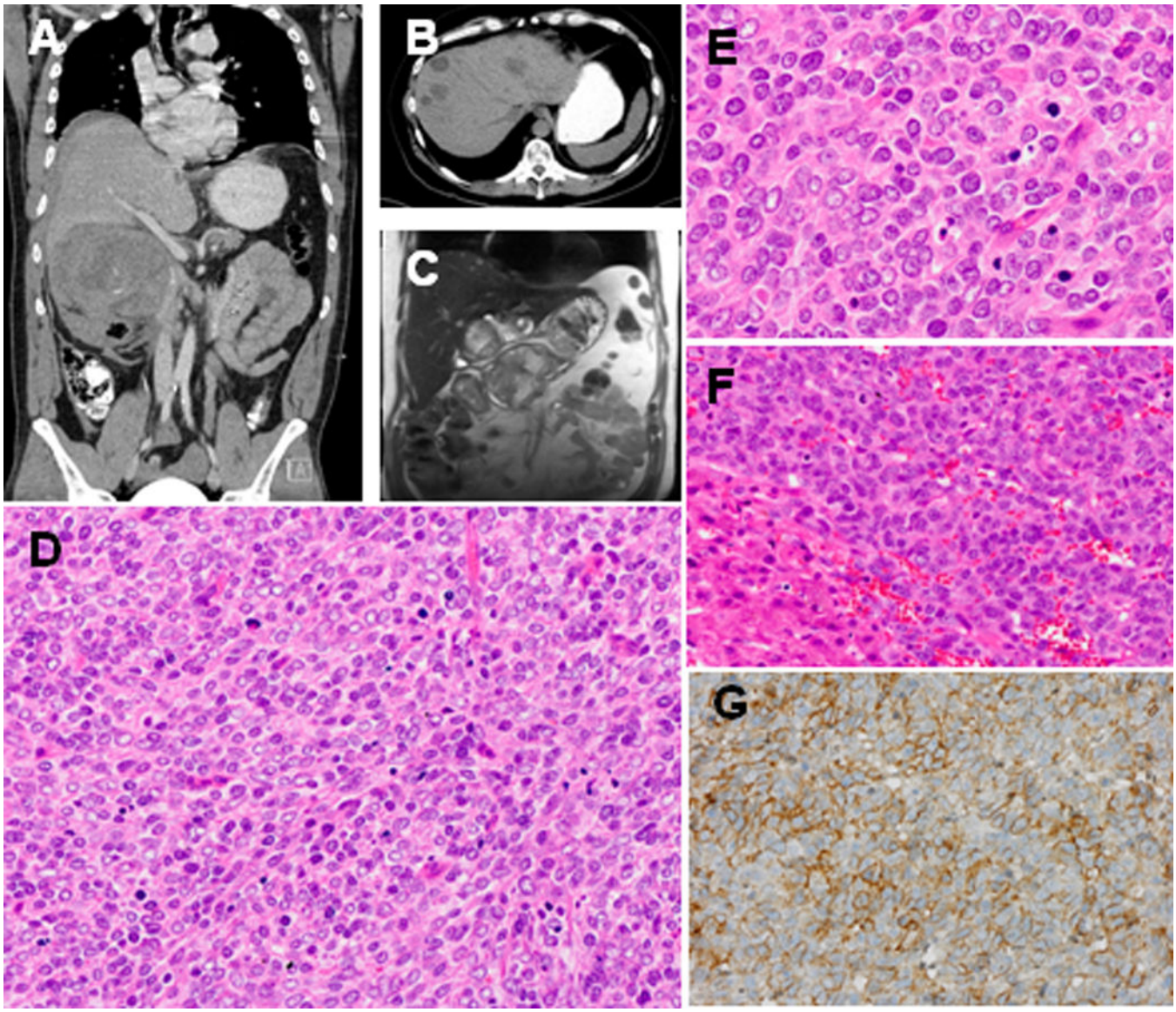

Figure 1. Clinico-pathologic findings of the index SBRCT1 with *BCOR-MAML3* fusion

Abdominal CT scan at presentation (A) showing a large intra-abdominal mass in the subphrenic/ subhepatic region, and after 19 months documenting rapid progression, with widespread metastases in the liver and peritoneum despite intensive chemotherapy and radiotherapy therapy (B,C). Morphologic appearance showing sheets of primitive round to ovoid cells set in a slightly collagenized stroma (D), with relatively uniform nuclei with fine stippled chromatin, eosinophilic scant cytoplasm, and a high mitotic rate (E); remained unchanged after chemo (F); with diffuse and strong membranous CD99 positivity (G).

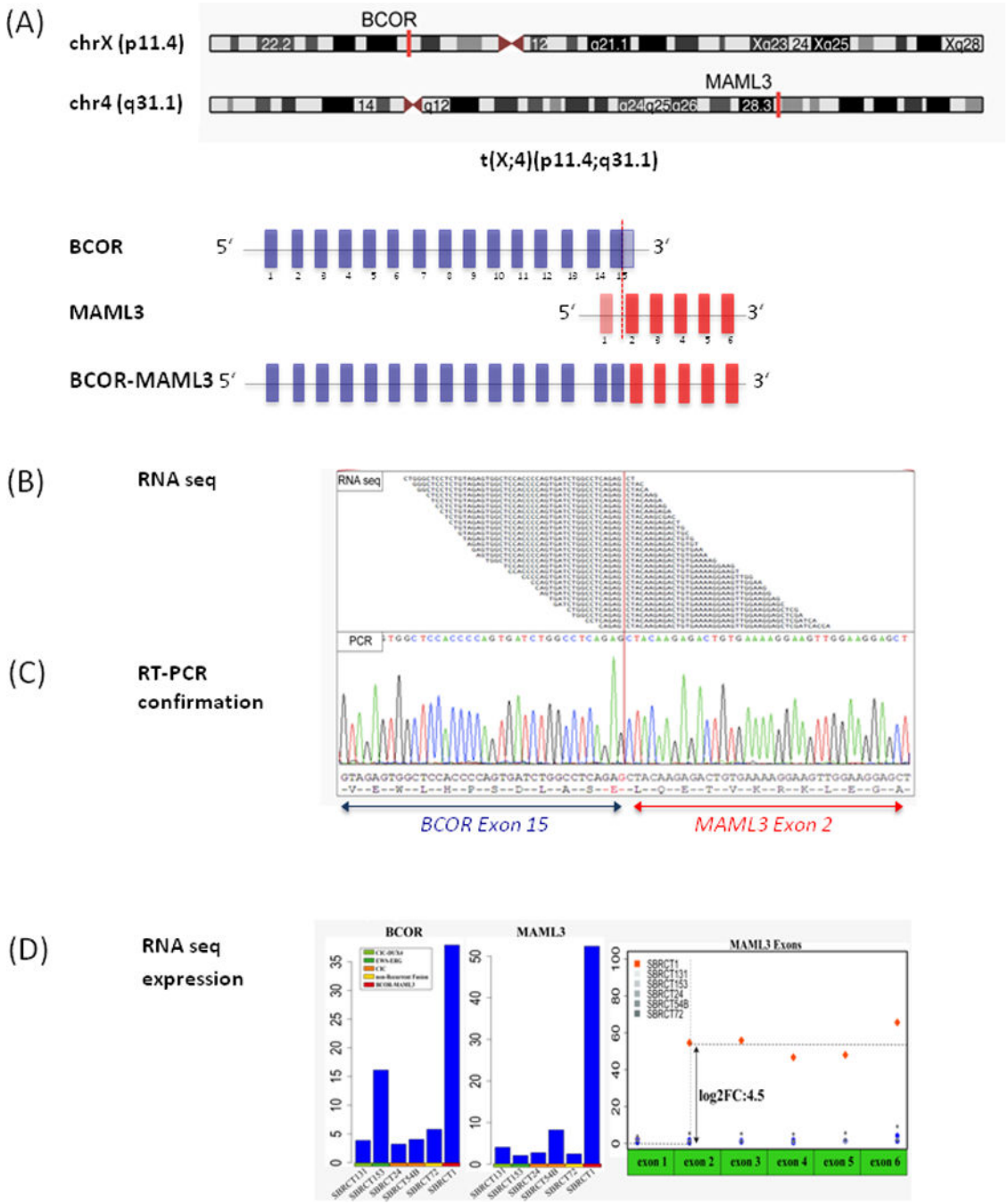

Figure 2. *BCOR-MAML3* gene fusion discovery and experimental validation (SBRCT1)

(A) Schematic representation of the *BCOR-MAML3* fusion indicating the chromosomal loci and exonic structure of the candidate transcript; (B) Alignment of the RNA reads covering the fusion junction detected by Fusion Seq algorithm; (C) RT-PCR validation demonstrates the junction sequence spanning *BCOR* exon 15 and *MAML3* exon 2; (D) Significant *BCOR* and *MAML3* mRNA upregulation noted by RNA sequencing, compared to other translocation positive SBRCTs (left panels, including *EWSR1-ERG*, *CIC-DUX4* fusions); as predicted from the structure of the chimeric *BCOR-MAML3* fusion, exons 2–6 of *MAML3*

showed differential overexpression compared to *MAML3* exon 1 in SBRCT1 compared to other translocation positive sarcomas (right panel).

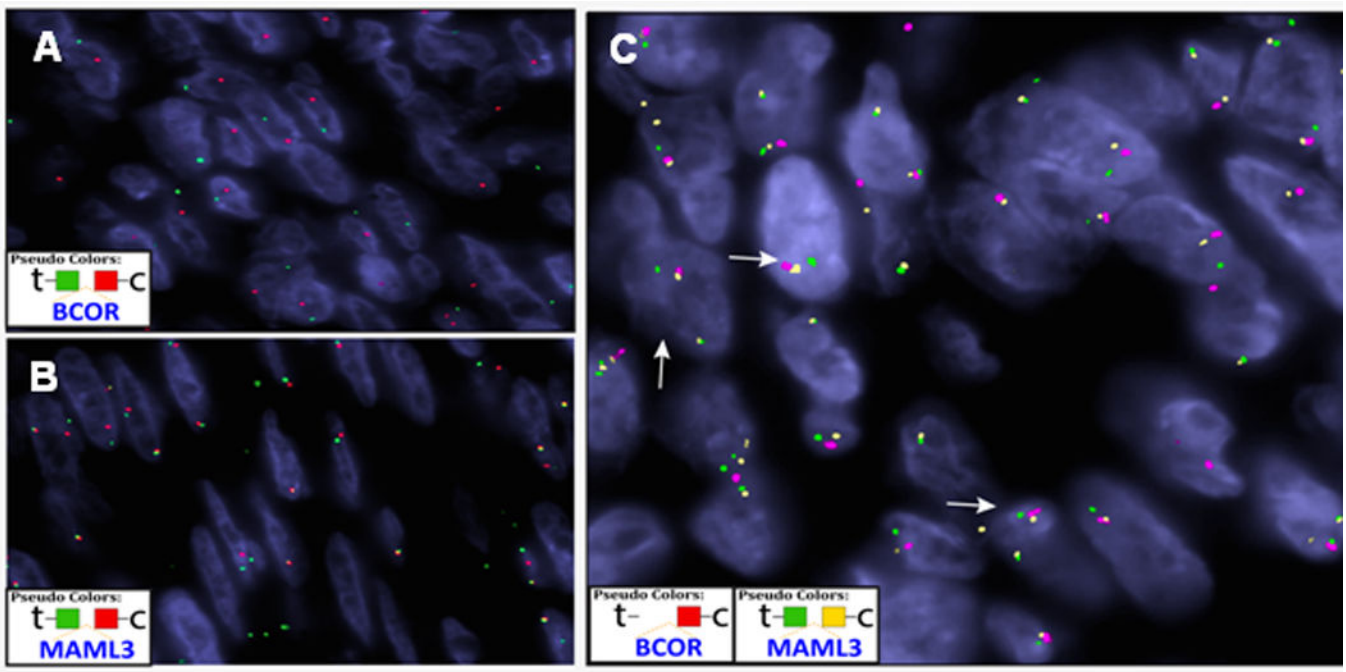

Figure 3. FISH detection of *BCOR-MAML3* fusion (SBRCT2)

Break-apart assay showing a split signal in *BCOR* (A) and in *MAML3* (B) (A,B: green telomeric, red centromeric); Three-color fusion FISH assay showing co-localization of *BCOR* (red) with *MAML3* (yellow, centromeric) and the *MAML3* split of the green (telomeric) and yellow (centromeric) (C).

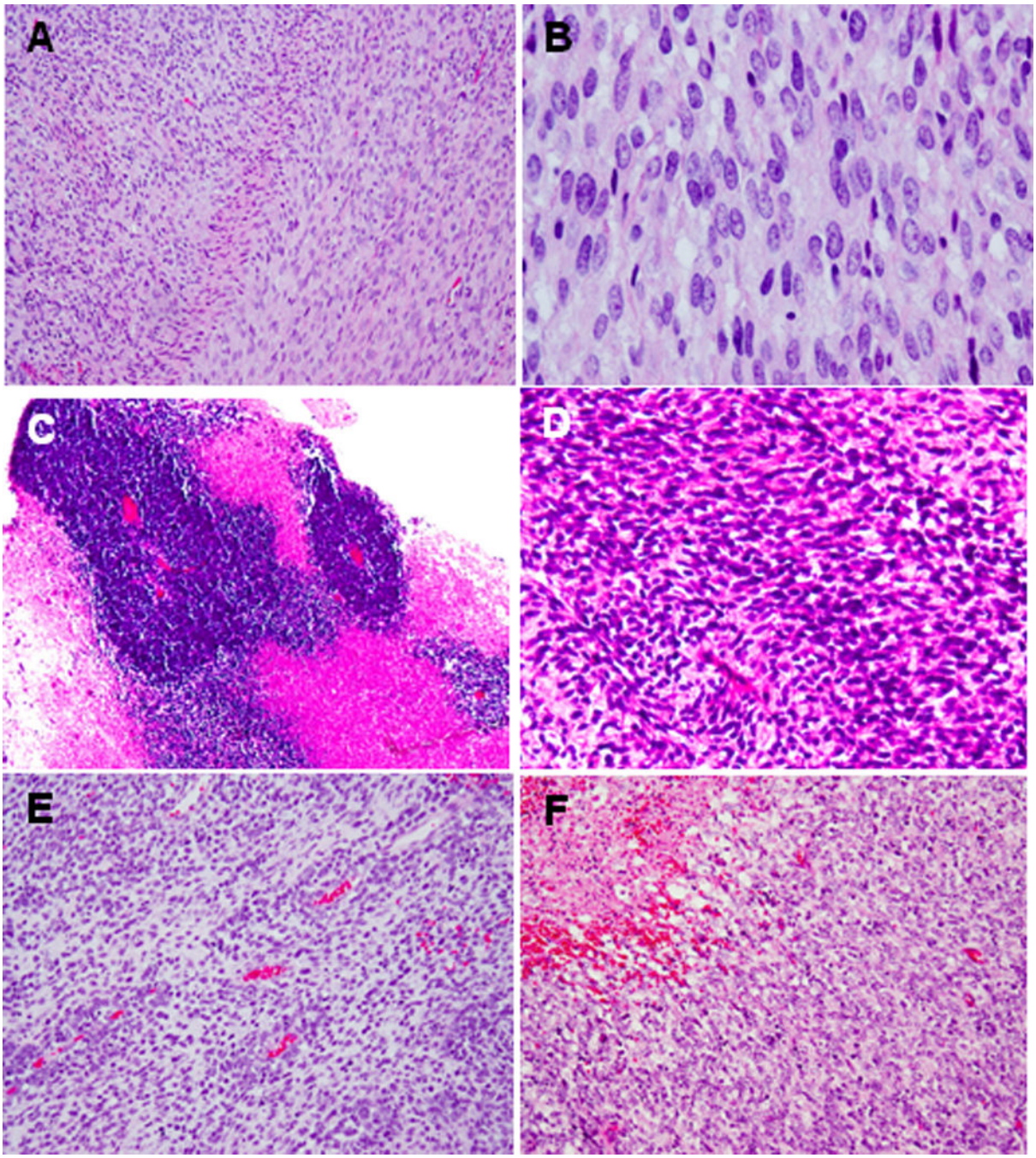

Figure 4. Morphologic spectrum of *BCOR* rearranged SBRCTs

Areas of spindling arranged in long fascicles or herring-bone pattern, which at high power shows ill-defined cell borders, ovoid nuclei with stippled chromatin (A,B: SBRCT2, *BCOR-MAML3*-positive); geographic areas of necrosis and areas of spindled morphology (C,D: SBRCT4, *ZC3H7B- BCOR* fusion). Monomorphic proliferation of round to oval cells showing a vague streaming pattern in a predominantly myxoid background (E, SBRCT7); primitive round cell morphology and geographic necrosis (F, SBRCT8).

Table 1

Clinical Features of *BCOR*-Rearranged SBRCTs (excluding *BCOR-CCNB3* positive SBRCT)

Case	Fusion/ Rearrangemen	Age/	Location sex	Tumor	Treatment size	Local recurrence/ metastatic disease	Outcome (mo)
1	*BCOR-MAML3*	44/M	Peritoneum (ST)	28 cm	CTX (V,I,D,E) & RT	LR & hepatic and peritoneal mets	DOD (19 mo)
2	*BCOR-MAML3*	7/M	Ilium (B)	8.4 cm	CTX & RT	LR	AWD (33 mo)
3	*ZC3H7B-BCOR*	57/F	Pelvic mass (ST)	11 cm	Partial resection	Recent case	N/A
4	*ZC3H7B-BCOR*	42/M	Arm (ST)	6.3 cm	CTX (VAC), RS	LR (2x), Mets (B, pancreas)	DOD (60 mo)
5	BCOR only	15/M	Leg (ST)	7 cm	NA	NA	NA
6	*BCOR* only	36/M	Groin/thigh (ST)	9 cm	CTX (D,TH-210)	Mets (LN, lung, B)	NA
7	*BCOR* only	5/M	Skull base (B)	NA	NA	NA	NA
8	*BCOR* only	70/M	Lung	11 cm	Resection	Mets(lung and B)	NA

M, male; F, female; B, bone; ST, soft tissue; CTX, chemotherapy; A, adriamycin; C, cyclophosphamide; D, doxorubicin; E, etoposide, I, ifosfamide; V, vincristine; RT, radiotherapy; AWD, alive with disease; DOD, died of disease; LN, lymph node; LR, local recurrence; Met, metastatic disease; NA, not available.

Table 2

Immunohistochemistry of *BCOR* rearranged SBRCTs

Case	Fusion	CD99	Cytokeratins	S100	Desmin	WT-1
1	*BCOR-MAML3*	pos (+++)	neg	neg	neg	neg
2	*BCOR-MAML3*	pos (+)	na	neg	neg	neg
3	*BCOR-ZC3H7B*	pos (+)	neg	neg	neg	neg
4	*BCOR-ZC3H7B*	pos (+)	neg	neg	na	na
5	*BCOR*	pos (+)	neg	neg	neg	na
6	*BCOR*	pos (+)	pos	na	neg	na
7	*BCOR*	neg	neg	neg	pos (focal)	neg
8	*BCOR*	na	neg	na	na	na

Table 3

Comparative clinical features of SBRCTs with *BCOR* abnormalities

	BCOR-Rearranged **(n=8)**	***BCOR-CCNB3*** **(n=11; present study)**	***BCOR-CCNB3*** **(n=42; meta-analysis)**
Gender (M:F)	7:1	10:1	32:10
Median age (y)	39	15	13
Age range (y)	5–70	2–44	5.9–25.6
Location			
Bone	2	9	29
Soft Tissue	3	2	13
I-abdominal/pelvic	2	0	0
Visceral	1	0	0